Cell PRESS
Open ACCESS

EXTENDED EXPERIMENTAL PROCEDURES

Myotube Differentiation and Metabolic Labeling

C2C12 mouse myoblasts were grown to near confluence then switched to media containing 2% dialyzed FBS (Invitrogen). During differentiation, cells were metabolically labeled using established methods (Ong et al., 2002; Ong and Mann, 2006). Briefly, cells were grown in Lys and Arg dropout medium supplemented with $^{12}C_6$-Lys and $^{12}C_6$-Arg or $^{13}C_6$-Lys and $^{13}C_6$-Arg, and after 3 days of differentiation, cells were infected with an adenovirus expressing either green fluorescent protein (GFP) or GFP tagged PGC-1α (GFP-PGC-1α) as previously described (Wu et al., 1999). Alternatively, cells were labeled with $^{12}C_6$-Lys and $^{12}C_6$,$^{14}N_4$-Arg, $^{12}C_6$-Lys and $^{13}C_6$,$^{14}N_4$-Arg or $^{12}C_6$-Lys and $^{13}C_6$,$^{15}N_4$-Arg, and after 3 days were infected with an adenovirus expressing GFP or GFP-PGC-1α ± DFO treatment as indicated. Three days following infection, cells were washed with PBS and processed for microarray or protein mass spectrometry. Experiments were performed in biological duplicate.

Primary Mouse Satellite Cell Media Formulation

80% Ham's F-10 Nutrient Mix (Invitrogen)
20% FBS (Invitrogen)
1 × GlutaMAX (Invitrogen)
2.5 ng/mL FGF-basic, human (added fresh to 50 ml aliquot) (Sigma-Aldrich)
10 ng/mL EGF, human (Sigma-Aldrich)
1 μg/mL insulin (Sigma-Aldrich)
0.5 mg/mL fetuin (added fresh to 50 ml aliquot) (Sigma-Aldrich)
0.4 μg/mL dexamethasone (Sigma-Aldrich)
1 × Antibiotic/Antimycotic (Invitrogen)

Mass Spectrometry

100 μg of protein lysate from each SILAC state was combined and resolved on 1D-SDS-PAGE (Nupage, Invitrogen). Gel lanes were cut into nine (GFP versus GFP-PGC-1α) or ten (triple encoding SILAC GPF versus GFP-PGC-1α ± DFO) slices. The gel slices from the latter group were acetylated in-gel (Thevis et al., 2003) before trypsin digestion to minimize trypsin digestion after lysine residues and improve SILAC-Arg quantification. Proteins were digested with a standard in-gel trypsin digestion protocol (Ong and Mann, 2006). Peptides were desalted off-line with C18 StageTips (Rappsilber et al., 2007) and analyzed with nanoESI-LC-MS using an Agilent 1100 (Santa Clara, CA) nanoflow pump and LTQ-Orbitrap (Thermo, Bremen). Peptides were separated on a C18 reversed phase column measuring 75 μm by 10 cm column with a 15 μ tip pulled in-house with a P2000 laser puller (Sutter, Novato CA) and packed with 3 μm Reprosil C18-aq beads (Dr. Maisch, Germany). Solvents A and B were 0.1% formic acid (Fluka, Germany) in water (HPLC grade, J.T. Baker) and 0.1% formic acid in 90% acetonitrile and 10% water, respectively. Peptides were eluted with a 90 min gradient of increasing acetonitrile (5% to 40% B) and analyzed with a data-dependent experiment selecting Top 3 most intense precursors for a CID MS/MS experiment in the linear ion trap. Raw files were processed for protein identification and SILAC quantification using MaxQuant ver. 1.2.0.18 with the appropriate SILAC mass modifications. The IPI mouse FASTA ver. 3.68 database plus common contaminants (MaxQuant) was used for database search with fixed modifications of carbamidomethylated cysteines and variable modifications of oxidized methionines, acetylated protein N-termini and lysines. Peptides containing up to two missed cleavages and a maximum of three SILAC labels per peptide were considered. Peptide mass tolerances were 20 ppm at the MS precursor level and 0.5 Da for MS/MS peptide data. Protein and peptide FDR rates were 1% and a minimum of 2 quantified peptides for each protein ratio was required.

Analysis of Mitochondrial Morphology

Following DFO treatment, mitochondrial morphology was analyzed in live MCH58 cells stained with 100 nM MitoTracker Red CMXRos (Invitrogen) for 30 min at 37°C and 5% CO_2. The stained cells were observed at 60 × magnification with an Olympus IX81 microscope and fluorescent images were captured with a Hamamatsu C4742-95-12G04 digital camera.

Primers Used for SYBR Green RT-qPCR

SYBR green primers were designed using the Roche Universal ProbeLibrary Assay Design Center tool.

Rplp0: left, actggtctaggacccgagaag; right, tcccaccttgtctccagtct
*Tfrc:*left, tcctttccttgcatattctgg; right, ccaaataaggatagtctgcatcc
Ppargc1b: left, gacgtggacgagctttcact; right, gagcgtcagagcttgctgtt
Ppargc1a: left, gaaagggccaaacagagaga; right, gtaaatcacacggcgctctt
Ndufs8: left, ttgcctgcaaactctgtgag; right, catcggctcttggctcag

Lysis Buffer Compositions

For immunoblotting, protein lysates were prepared in RIPA buffer composed of 150 mM NaCl, 1% IGEPAL CA-630, 0.5% sodium deoxycholate, 0.1% SDS, 50 mM Tris (pH 8.0), 0.4 mM EDTA (pH 8.0), 10% glycerol and a protease inhibitor cocktail (Roche Diagnostics).

For ferroportin experiments, the lysis buffer consisted of 150 mM NaCl, 1% Triton X-100, 10 mM Tris (pH 7.4), 10 mM EDTA (pH 8.0) and a protease inhibitor cocktail (Roche Diagnostics).

Post Assay Cell Quantitation

Cell number was quantified post-MitoTracker quantitation and XF analysis by crystal violet staining as previously described. (Kueng et al., 1989). Briefly, cells were fixed with 10 μl of 11% glutaraldehyde added to 100 μl of medium. Following a 15 min incubation, the plates were washed by submersion in diH_2O, air-dried and stained with 100 μl of 0.1% crystal violet. After a 20 min incubation, the plates were washed to remove excess dye and were air-dried. Bound dye was solubilized with 100 μl of 10% acetic acid and the absorbance was measured at 590 nm using a BioTek Synergy 2 Microplate Reader.

SUPPLEMENTAL REFERENCES

Kueng, W., Silber, E., and Eppenberger, U. (1989). Quantification of cells cultured on 96-well plates. Anal. Biochem. *182*, 16–19.

Ong, S.E., Blagoev, B., Kratchmarova, I., Kristensen, D.B., Steen, H., Pandey, A., and Mann, M. (2002). Stable isotope labeling by amino acids in cell culture, SILAC, as a simple and accurate approach to expression proteomics. Mol. Cell. Proteomics *1*, 376–386.

Rappsilber, J., Mann, M., and Ishihama, Y. (2007). Protocol for micro-purification, enrichment, pre-fractionation and storage of peptides for proteomics using StageTips. Nat. Protoc. *2*, 1896–1906.

Thevis, M., Ogorzalek Loo, R.R., and Loo, J.A. (2003). In-gel derivatization of proteins for cysteine-specific cleavages and their analysis by mass spectrometry. J. Proteome Res. *2*, 163–172.

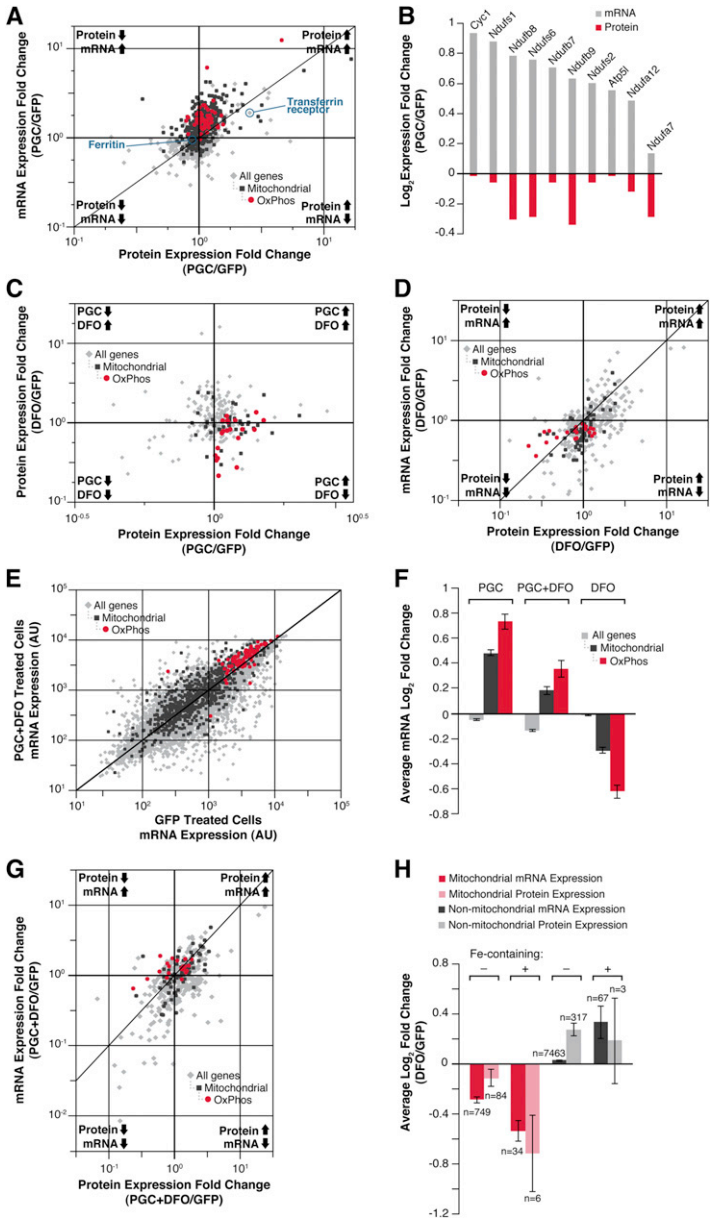

Figure S1. Large-Scale Analyses of mRNA and Protein Abundance Reveal a Widespread Role for Iron in Mitochondrial Biogenesis, Related to Figure 1

Differentiated C2C12 mouse myotubes were analyzed after 3 days of PGC-1α overexpression and/or 100 μM DFO treatment.

(A) Relationship between PGC-1α induced changes in protein and mRNA expression (all genes, $r_s = 0.41$, $p = 5.7 \times 10^{-52}$; mitochondrial genes, $r_s = 0.53$, $p = 1.9 \times 10^{-30}$; Spearman's rank correlation test).

(B) Changes in OxPhos mRNAs and proteins showing discordance in expression during PGC-1α overexpression.

(C) Comparison of PGC-1α and DFO induced changes in protein expression (50% of mitochondrial proteins versus 27% of all proteins are in the lower right quadrant, $p = 2.2 \times 10^{-6}$, χ^2 contingency test).

(D) Relationship between DFO induced changes in protein and mRNA expression (all genes, $r_s = 0.58$, $p = 8.8 \times 10^{-35}$; mitochondrial genes, $r_s = 0.58$, $p = 2.5 \times 10^{-9}$; Spearman's rank correlation test).

(E) Comparison of mRNA expression in GFP treated cells and PGC-1α+DFO treated cells (AU, arbitrary units).

(F) Comparison of the average PGC-1α, PGC-1α+DFO and DFO induced changes in transcript levels for the indicated groups. Data are displayed as mean ± SEM.

(G) Relationship between PGC-1α+DFO induced changes in protein and mRNA expression (all genes, $r_s = 0.54$, $p = 6.8 \times 10^{-29}$; mitochondrial genes, $r_s = 0.60$, $p = 4.4 \times 10^{-10}$; Spearman's rank correlation test).

(H) Comparison of average DFO induced changes to transcript and protein levels for the indicated groups. The sample size (n) is indicated. Data are displayed as mean ± SEM.

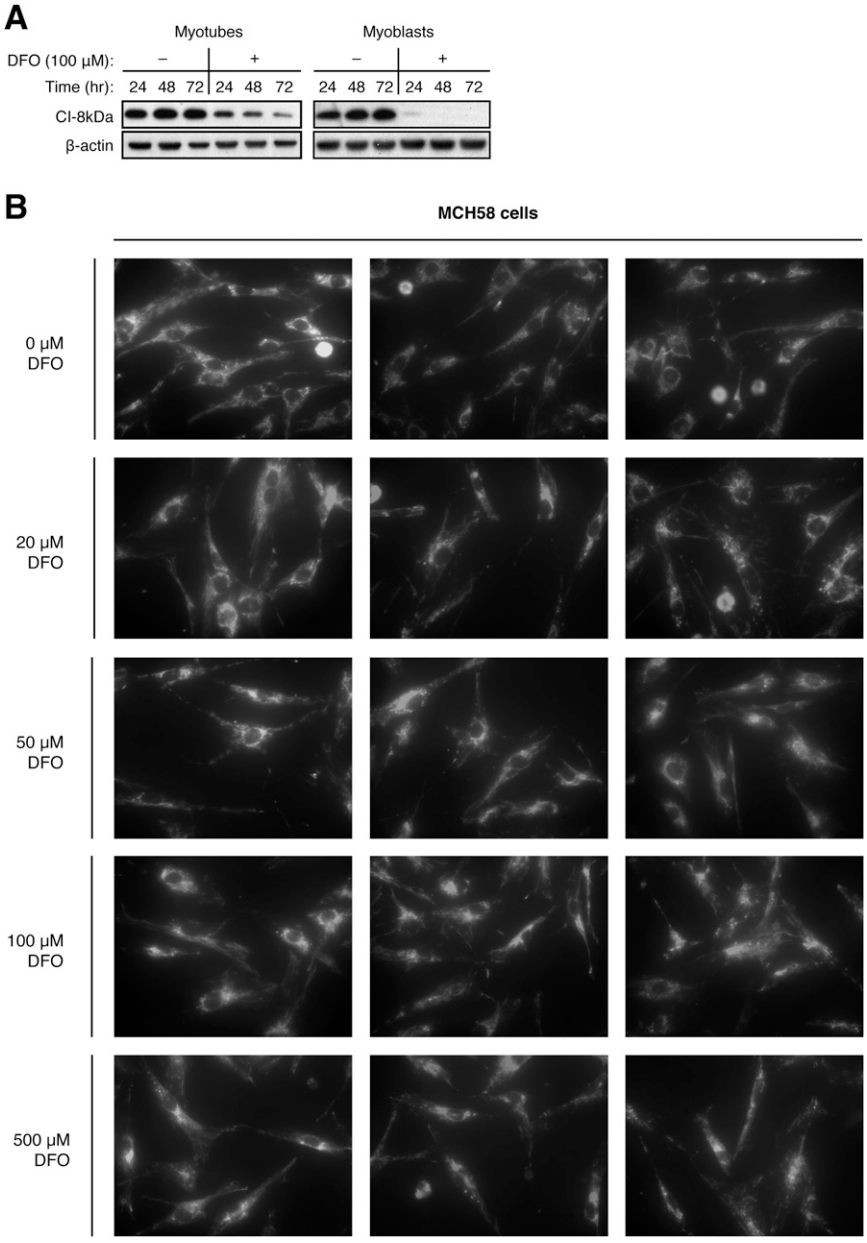

Figure S2. Iron Chelation Causes a Specific Remodeling of Mitochondrial Content, Related to Figure 2

(A) Level of the indicated proteins after DFO treatment for the indicated times in C2C12 myotubes and myoblasts as assessed by immunoblotting.

(B) MitoTracker Red CMXRos staining of live MCH58 cells treated with the indicated concentrations of DFO for 24 hr (three replicates per DFO concentration are shown).

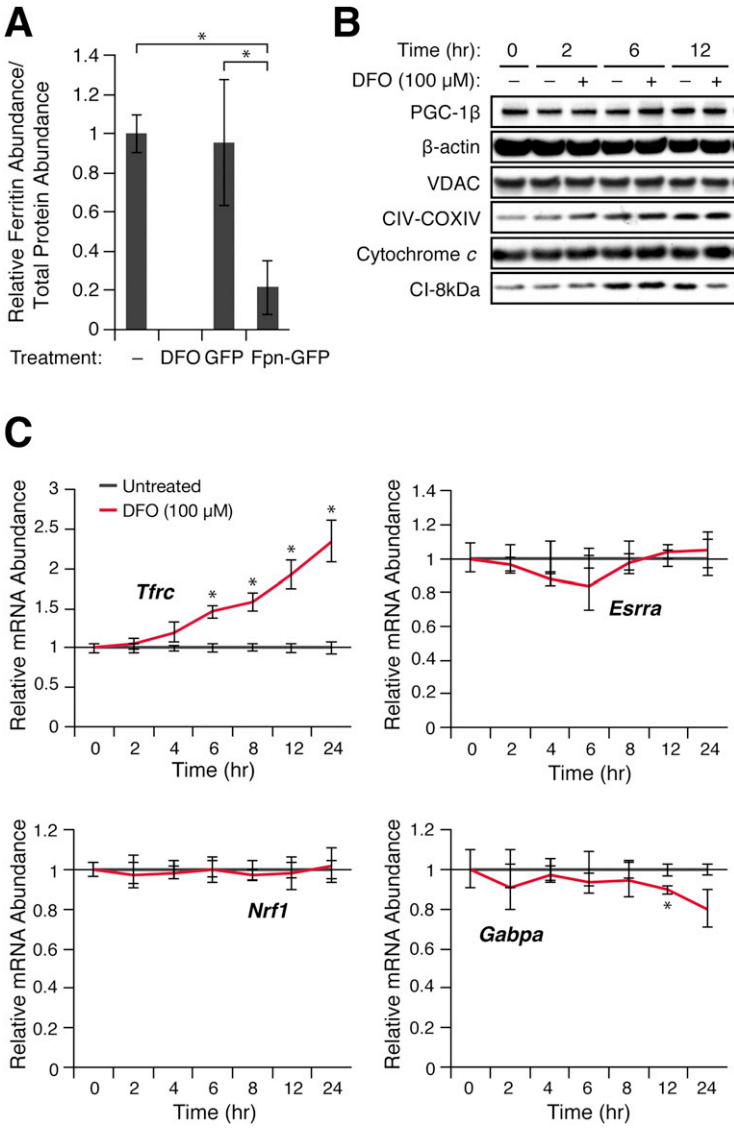

Figure S3. Time Course Expression Analysis of Mitochondrial Genes, Mitochondrial Biogenesis-Related Transcription Factors, and Co-activators during Iron Deprivation, Related to Figure 3

(A) Ferritin protein abundance/total protein abundance in HEK293 cells after 100 μM DFO treatment or ferroportin (Fpn-GFP) overexpression for 48 hr as determined by ELISA. Data are displayed as mean ± SD of triplicate measurements (*$p < 0.05$, ANOVA with Tukey's test).

(B) Level of the indicated proteins in C2C12 myoblasts following DFO treatment for the indicated times as assessed by immunoblotting.

(C) Abundance of *Tfrc*, *Esrra*, *Nrf1,* and *Gabpa* in myoblasts following DFO treatment for the indicated times as assessed by real-time qPCR. Data are displayed as mean ± SD of triplicate measurements (*$p < 0.05$, Student's t test).

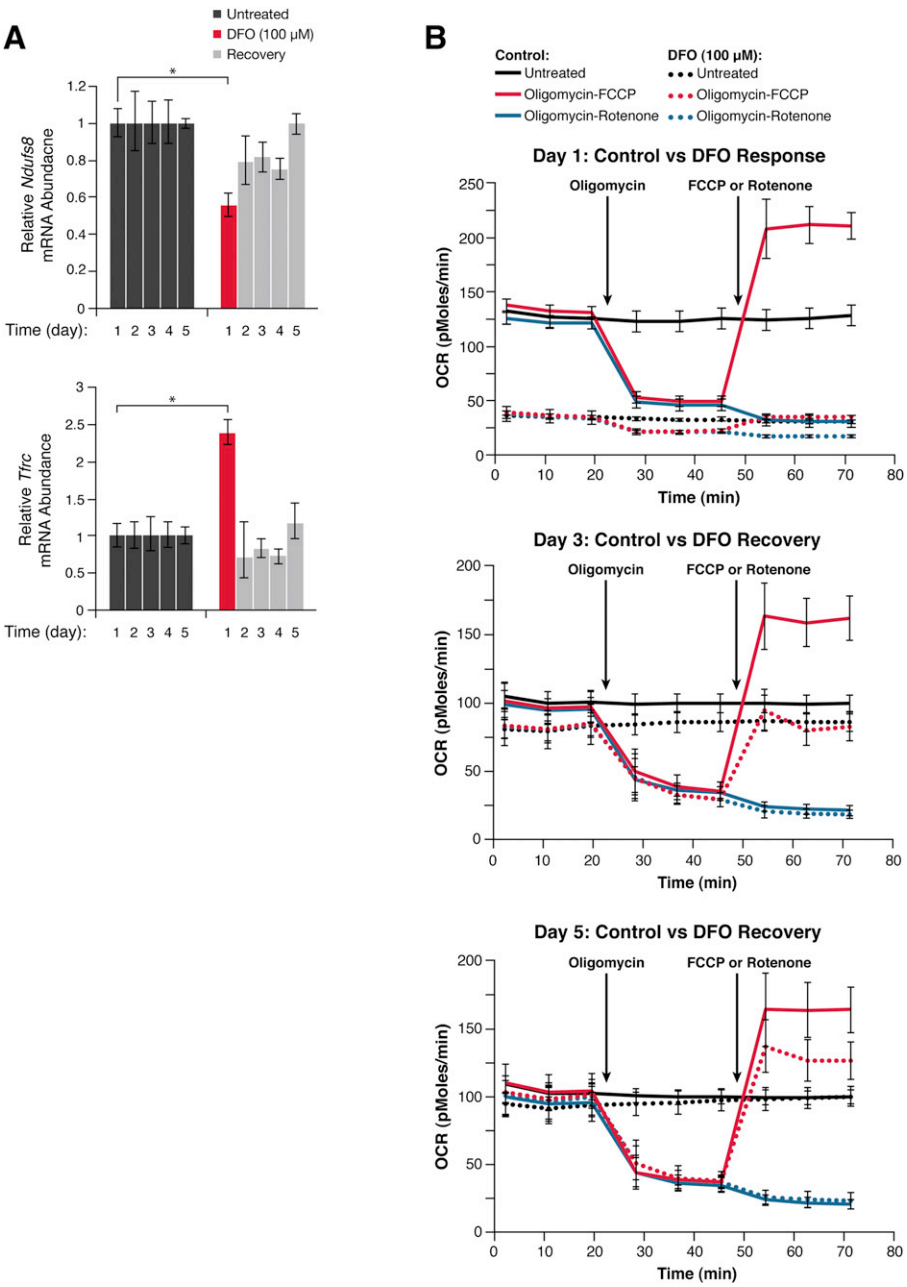

Figure S4. Iron Deprivation Causes a Universal and Reversible Reduction in Mitochondrial Protein Levels and Respiratory Function, Related to Figure 4

(A) Abundance of *Ndufs8* and *Tfrc* in C2C12 myoblasts during DFO response and recovery as assessed by real-time qPCR. Data are displayed as mean ± SD of triplicate measurements (*$p < 0.05$, Student's t test).

(B) Mitochondrial respiratory profiles of myoblasts treated with DFO for 24 hr then passaged every 24 hr in DFO free media. OCR was measured after 24 hr of DFO treatment (day 1), then 48 hr (day 3) and 96 hr (day 5) following the passage of DFO treated myoblasts into DFO-free media. Data are displayed as mean ± SD of 14-16 replicates. Spare respiratory capacity was calculated by dividing the maximal rate after FCCP injection by the basal rate (third basal measurement before the first injection) with the minimal rate after the rotenone injection subtracted from each of these rates. Coupling efficiency was calculated as 1 minus the quotient of the minimal rate after oligomycin injection divided by the basal rate with the minimal rate after the rotenone injection subtracted from each of these rates.